

COHERENT PHOTOPRODUCTION OF THE  $\eta^0$  MESON FROM DEUTERIUM\*

R. L. Anderson

Stanford Linear Accelerator Center, Stanford, California 94305

and

R. Prepost†

Department of Physics and High Energy Physics Laboratory, Stanford University, Stanford, California 94305

(Received 16 May 1969)

The isoscalar part of the  $\eta^0$  photoproduction amplitude near threshold has been determined by differential cross-section measurements of the coherent process  $\gamma+d \rightarrow \eta^0+d$  from near threshold to 150 MeV above threshold. By comparison of the results with earlier measurements of  $\gamma+p \rightarrow \eta^0+p$  and a recent measurement of  $\gamma+d \rightarrow \eta^0+(p,n)$  it is possible to argue that the isovector part of the  $\eta^0$  photoproduction amplitude near threshold is much smaller than the isoscalar part and is consistent with zero.

Eta photoproduction near threshold is dominated by the S-wave,  $J=\frac{1}{2}$ ,  $I=\frac{1}{2}$ , mass-1550-MeV, odd-parity baryon resonance. A determination of the isospin character of the electromagnetic transition moments from the nuclear ground state is desirable for detailed tests of various theoretical approaches, such as photoproduction sum rules and various symmetry and quark schemes. Toward this end, studies of the reactions  $\gamma+d \rightarrow \eta^0+d$ ,  $\gamma+d \rightarrow \eta^0+(p,n)$ , and  $\gamma+p \rightarrow \eta^0+p$  can be used to make a determination of the relative isovector and isoscalar couplings. Specifically, since both the deuteron and the eta meson are isoscalar particles, only the isoscalar part of the  $\langle \eta^0 N | j | N \rangle$  matrix element can contribute to the coherent production from the deuteron. This Letter describes a measurement of the differential cross section for the reaction  $\gamma+d \rightarrow \eta^0+d$  near  $90^\circ$  in the c.m. system from threshold to approximately 150 MeV above threshold in approximately 20-MeV steps. These measurements were made using counter techniques at the Stanford University 1.1-GeV linear electron accelerator.

Observation of  $\eta^0$  production in the reaction  $\gamma+d \rightarrow \eta^0+d$  has been accomplished by detecting the recoil deuteron. Since this process has a two-body final state, a measurement of the deuteron momentum and angle is sufficient to uniquely determine the incident photon energy. The electron beam is brought out into the experimental end station and passes through three secondary-emission monitors, a beam-position monitor, and a fast torid. The electron beam itself consists of pulses occurring at 23.0 Mc/sec, each less than 1 nsec in width during an overall machine-pulse width of 1  $\mu$ sec. This "chopped" beam is prepared by passing the electron beam between a set of plates near the accelerator gun

to which an 11.5-Mc/sec rf voltage is applied. Immediately after the deflection plates, a collimator is positioned on the accelerator axis thus producing the "chopped" beam. This time structure in the beam is then used for a time-of-flight time marker in order to measure the time-of-flight distribution of particles traversing a magnetic spectrometer.

The electron beam passes through a 0.03-radiation-length foil and is then deflected by a sweeping magnet. After collimation, the photon beam then passes through a liquid-deuterium target. The beam position is monitored once more after the deuterium target, and then the photon-beam energy is measured in a secondary-emission quantameter.

The spectrometer used to detect the recoil deuterons is a 44-in. radius,  $90^\circ$  bend,  $n=0$  type magnet which is capable of 0.1% momentum resolution up to 700 MeV/c. The detecting counters consist of seven 1% momentum-defining counters and two focal-plane defining counters.

Deuterons are identified by range, energy-loss, and time-of-flight requirements. Under most experimental conditions the proton flux was some 100 times more intense than the deuteron flux. Under normal experimental conditions, the time-of-flight requirement is set for deuterons and the resultant deuteron signal has less than a 1% proton contamination.

The procedure used for the cross-section measurements is similar to that used by Prepost, Lundquist, and Quinn to measure the cross section for  $\gamma+p \rightarrow \eta^0+p$ .<sup>1</sup> For a fixed spectrometer momentum and angle setting, the deuteron yield is measured as a function of primary electron energy. As the electron energy increases (i.e., the bremsstrahlung end-point energy) the counter yields will increase when the threshold ener-

gy for a new process is reached. In particular, if the process has a two-body final state, the counter yields will rise at the threshold energy and trace out a bremsstrahlung curve for fixed photon energy and variable end-point energy. This yield reaches an approximately constant value some 30 MeV above the threshold for the reaction. On the other hand, if the reaction has a three-body final state such as  $\gamma + d \rightarrow \pi^+ + \pi^- + d$ , then a measurement of the deuteron momentum and angle is not sufficient to identify the photon energy, and the yield continues to rise above the threshold with a contribution from all photon energies from the laboratory threshold energy to the bremsstrahlung end-point energy. Our procedure has been to trace out the deuteron yield as a function of energy from the threshold for  $\gamma + d \rightarrow \pi^0 + d$  to approximately 150 MeV above the threshold for  $\gamma + d \rightarrow \eta^0 + d$ . Figure 1 shows two examples of such yield curves which show a signal due to  $\gamma + d \rightarrow \eta^0 + d$ . The process  $\gamma + d \rightarrow \gamma + d$  is too small to be seen against the much larger signal from  $\gamma + d \rightarrow \pi^0 + d$ . The energy interval steps are approximately 10 MeV and vary somewhat for the various experimental points. As the yield curves are continued beyond  $\pi^0$  threshold, the next kinematically allowed process is  $\gamma + d \rightarrow 2\pi + d$ . The yield then continues to rise as the bremsstrahlung end-point energy is increased and this is the major background for  $\eta^0$  production. The curves clearly show the expected increase in deuteron yield corresponding to  $\eta^0$  production. The arrows indicate the expected threshold energy at the center of the momentum acceptance. The yields show the expected behavior, which is a leveling off of the yield due to  $\eta^0$  production some 30 to 40 MeV above the threshold energy.

In order to determine the  $\eta^0$  differential cross sections from the measured yields, the height of the deuteron step must be determined and this makes it necessary to extrapolate the two-pion yields from below the  $\eta^0$  threshold where they are measured directly, to above the  $\eta^0$  threshold where the yields are the sum of an  $\eta^0$  signal and a two-pion yield. There is also, of course, a constant contribution from  $\pi^0$  production. We have found that both a phase-space polynomial and a linear function are a good representation for the energy dependence of the data in the vicinity of the  $\eta^0$  threshold.

The actual interval which is fitted is the region 100 MeV below the  $\eta^0$  threshold and a 100-MeV interval which starts 50 MeV above the  $\eta^0$  thresh-

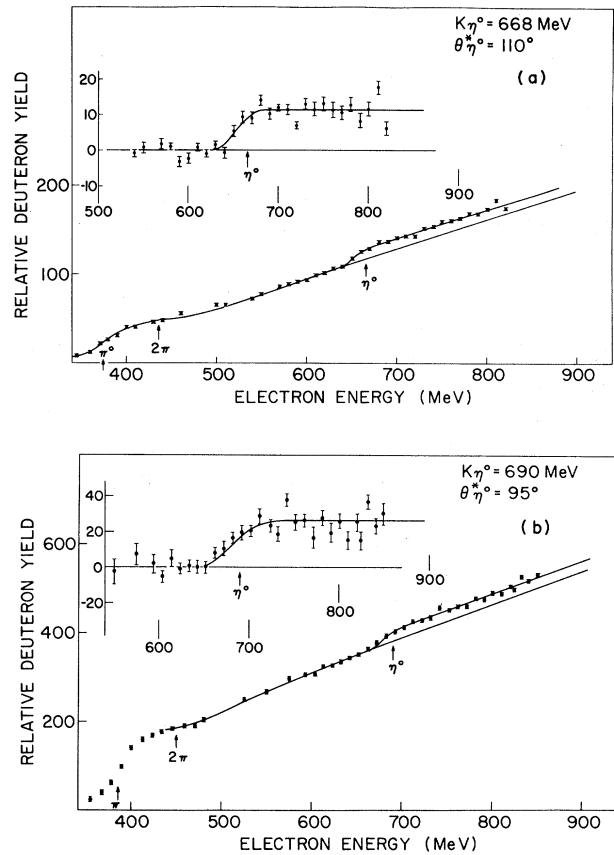


FIG. 1. (a), (b) Two deuteron yield curves showing a signal due to  $\eta^0$  production. The inserts in the upper left corner show the yields in the vicinity of  $\eta^0$  threshold with backgrounds subtracted.

old. In Fig. 1, the solid line is drawn in as a representation to the actual least-squares curve. In this manner we obtain a least-squares solution for the height of the  $\eta^0$  step.

The inserts in Fig. 1 show the deuteron yields in the vicinity of the  $\eta^0$  threshold with the background processes subtracted. These background processes include single- $\pi^0$  production, two-pion production, and a small (10%) empty-target background. If the background has been subtracted properly, the remaining yield will have the shape of a bremsstrahlung curve for fixed photon energy. The main feature of this curve is that the yield must have a plateau some 30 to 40 MeV above threshold. The Fig. 1 yields have this feature as do our other experimental points.

The eta yields are converted into a differential cross section by normalizing to the deuteron yield where only deuterons accompanied by a  $\pi^0$  are produced, thus providing a normalization under the same laboratory momentum-transfer

and angle conditions. These data are available from the experiment of Friedman and Kendall<sup>2</sup> in the appropriate energy range but at somewhat lower momentum transfers. We have corrected these data to our momentum-transfer conditions by using the measured slope of the  $\gamma + d \rightarrow \pi^0 + d$  cross section as a function of momentum transfer. This slope is just the slope of the deuteron form factor and is quite well known.

We have measured such yield curves for six photon energies, which in the laboratory frame are 668, 690, 708, 715, 722, and 776 MeV. The threshold energy for  $\eta^0$  production is 629 MeV. All points were taken near  $\theta_{\eta^0}^* = 90^\circ$  in the c.m. system. The recoil momentum ranges from 564 to 663 MeV/c. The results for the c.m. differential cross section  $(d\sigma/d\Omega^*)_{\eta^0 d}$  are plotted in Fig. 2(a) as a function of c.m. momentum. All points have been normalized to a laboratory recoil momentum of  $\vec{q} = 590$  MeV/c. The errors in-

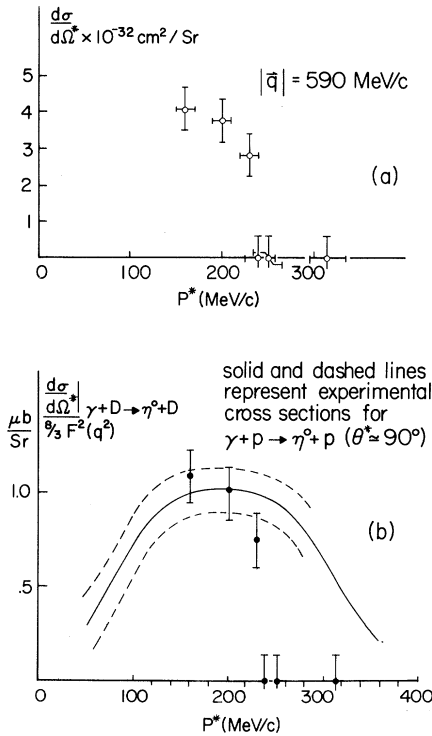


FIG. 2. (a) The differential cross section for the process  $\gamma + d \rightarrow \eta^0 + d$  in the c.m. system versus  $p^*$ , the c.m. final-state momentum. The c.m. meson angle is  $\approx 90^\circ$  and the points have all been normalized to the value of the deuteron form factor evaluated at  $q = 590$  MeV/c.  $F^2(590 \text{ MeV/c}) = 1.4 \times 10^{-2}$  was used. (b) The differential cross section for  $\gamma + d \rightarrow \eta^0 + d$  divided by  $(8/3) \times F^2(q^2)$  vs  $p^*$ . The measured cross sections for the reaction  $\gamma + p \rightarrow \eta^0 + p$  ( $\theta^* \approx 90^\circ$ ) are represented by the solid line.

clude both statistical and normalization uncertainties. The features of interest are the large cross section near threshold and the falloff with increasing c.m. momentum. This is very similar to the gross features seen in the cross-section measurements for  $\gamma + p \rightarrow \eta^0 + p$ .

The interpretation of these results is interesting primarily in relation to the process  $\gamma + p \rightarrow \eta^0 + p$ . This reaction has been studied near threshold by the Stanford<sup>1</sup> and Orsay<sup>3</sup> groups and at somewhat higher energies by the Frascati and California Institute of Technology groups.<sup>4</sup> The rapid rise from threshold together with the isotropic angular distribution show that the production is in an  $S_{1/2}$  or  $P_{1/2}$  state or a mixture of the two. Related experiments in the reaction  $\pi^- + p \rightarrow \eta^0 + n$  near threshold show a similar behavior. Theoretical considerations<sup>5</sup> have shown that the threshold behavior may be identified as an  $I = \frac{1}{2}$ ,  $S_{1/2}$  resonance ( $S_{11}$ ) with mass = 1500-1530 MeV.

The process  $\gamma + d \rightarrow \eta^0 + d$  may be related to  $\gamma + p \rightarrow \eta^0 + p$  and  $\gamma + n \rightarrow \eta^0 + n$  within the framework of the impulse approximation. The photoproduction amplitude may be separated into an isoscalar and isovector part, viz.,  $T = T^0 + \tau_3 T^+$  where  $T^0$  and  $T^+$  are the isoscalar and isovector parts of the single-nucleon amplitude, respectively, and  $\tau_3$  is the  $z$  component of the nucleon isospin operator. Only  $T^0$  contributes to the process  $\gamma + d \rightarrow \eta^0 + d$ , and the relevant photoproduction multipole for an  $S_{1/2}$  final state is therefore the isoscalar part of the  $E_{0+}$  electric-dipole amplitude. In the impulse approximation

$$\begin{aligned} \langle \eta^0 d | T_d^0 | \gamma d \rangle \\ = \int d^3 r e^{i q \cdot r / 2} \Psi_d(\mathbf{r}) [T_1^0 + T_2^0]_{av} \Psi_d(\mathbf{r}), \end{aligned}$$

where  $q$  is the laboratory recoil momentum,  $\mathbf{r}$  is the nucleon relative coordinate, and  $\Psi_d(\mathbf{r})$  is the deuteron wave function. The amplitude  $[T_1^0 + T_2^0]_{av}$  represents an average over the deuteron Fermi momentum distribution for the single-nucleon amplitudes. This has the effect of averaging over a range of photon energies. For an  $S_{1/2}$  final state this reduces to<sup>6</sup>  $|\langle \eta^0 d | T_d^0 | \gamma d \rangle|^2 = (8/3) \times |T^0|_{av}^2 F^2(q^2)$ , where  $F^2(q^2)$  is a deuteron structure function and is generally referred to as the effective form factor. For comparison, the corresponding amplitude for production from the proton is  $|\langle \eta^0 p | T | \gamma p \rangle|^2 = |T^0 + T^+|^2$ . Thus a measurement of  $\gamma + d \rightarrow \eta^0 + d$  determines the isoscalar amplitude if the deuteron form factor is independently known. The isovector amplitude may then be determined with the additional information pro-

vided by a measurement of incoherent production from the deuteron which is essentially just the sum of the cross sections from the free proton and neutron. The result of such an experiment has been recently reported by the Frascati group.<sup>7</sup> In terms of  $T^0$  and  $T^+$ , the differential cross sections for  $\gamma+d \rightarrow \eta^0+d$  and  $\gamma+p \rightarrow \eta^0+p$  are<sup>8</sup>

$$\frac{d\sigma}{d\Omega^*} \Big|_{\eta^0 d} \simeq \frac{1}{(4\pi)^2} \frac{8}{3} |T^0|_{av}^2 \left( \frac{P^*}{k_{\gamma-d^*}} \right)^2 F^2(q^2),$$

and

$$\frac{d\sigma}{d\Omega^*} \Big|_{\eta^0 p} = \frac{1}{(4\pi)^2} |T^0 + T^+|^2 \left( \frac{P^*}{k_{\gamma-d^*}} \right)^2,$$

where  $p^*$  and  $k^*$  are the final-state c.m. momentum and c.m. photon energy, respectively. Values for the form factor  $F^2(q^2)$  may be obtained from the impulse-approximation analysis of the measurements of Ref. 2 and may also be calculated directly from the deuteron wave function. These two methods agree well as long as one is working in a region where the meson rescattering corrections are small. The Frascati group has concluded that the  $\eta^0$  rescattering correction is small, from measurements on inelastic  $\eta^0$  photoproduction on various nuclei.<sup>7</sup>

In order to make a direct comparison of  $|T^0|_{av}$  and  $|T^0 + T^+|$  we have plotted in Fig. 2(b) the quantity

$$\frac{(d\sigma/d\Omega^*)_{\eta^0 d} \simeq d\sigma}{(8/3)F^2(q^2) d\Omega^*} \Big|_{\eta^0-N(\text{isoscalar})}$$

as a function of  $p^*$ , the c.m. momentum. The figure also includes as a solid line the average value of the measured cross sections for  $\gamma+p \rightarrow \eta^0+p$  taken from Refs. 1, 3, and 4. The approximate spread in experimental precision is shown by the dashed lines. It is convenient to plot the cross sections as a function of  $p^*$  since the phase-space factor is then kept the same for both reactions, and since the Fermi momentum distribution in the deuteron prevents a unique determination of the effective single-nucleon photon energy.

The conclusions of interest are as follows:

(1) Figure 2(a) shows that coherent  $\eta^0$  production from the deuteron is significant and measurable near threshold and falls off rapidly as a function of energy. The points at approximately 85 and 140 MeV above threshold do not show a measurable signal.

(2) Figure 2(b) shows that when the form-factor

dependence is removed from the cross sections, the resultant isoscalar cross section is comparable in size with the  $\gamma+p \rightarrow \eta^0+p$  cross section near threshold and shows a similar resonant behavior. This allows us to conclude that  $|T^0|_{av}^2 \simeq |T^0 + T^+|^2$  near threshold.

(3) The recent  $\eta^0$  production measurements from deuterium of Ref. 7 are dominated by incoherent production and allow one to conclude that  $\text{Re}(T^0 T^{+*}) \approx 0$ . Assuming that this result is valid over our photon energy range, and combining with (2) above, one can solve for  $|T^+|$  and therefore  $|T^+| \approx 0$ . This shows that the production near threshold is dominated by the isoscalar amplitude and that the isovector part is consistent with zero until ~80 MeV above threshold.

(4) If the threshold behavior of the  $\eta^0$  deuteron production is determined by the  $S_{11}$  (1550 MeV) isobar, then the photoproduction amplitude for this isobar is predominantly an isoscalar transition. One must, however, qualify this statement and keep in mind that the effective single-nucleon-photon invariant mass cannot be uniquely determined due to Fermi momentum smearing.

We would like to thank L. Boyer, J. Grant, and P. Zihlmann for their assistance with the experimental setup.

\*Work supported in part by the U. S. Office of Naval Research, Contract No. Nonr 225 (67), and in part by the U. S. Atomic Energy Commission under Contract No. AT(11-1)-881, COO-881-234.

†Now at Department of Physics, University of Wisconsin, Madison, Wis.

<sup>1</sup>R. Prepost, D. Lundquist, and D. Quinn, Phys. Rev. Letters **18**, 82 (1967).

<sup>2</sup>J. I. Friedman and H. W. Kendall, Phys. Rev. **129**, 2802 (1963).

<sup>3</sup>B. Delcourt, J. LeFrancois, J. P. Perez-y-Jorba, and G. Sauvage, Phys. Letters **29B**, 75 (1969).

<sup>4</sup>C. Bacci, R. Baldini-Celio, C. Mencuccini, A. Reale, M. Spinetti, and A. Zallo, Phys. Rev. Letters **20**, 571 (1968); E. D. Bloom, C. A. Heusch, C. Y. Prescott, and L. S. Rochester, Phys. Rev. Letters **21**, 1100 (1968).

<sup>5</sup>A. T. Davies and R. G. Moorhouse, Nuovo Cimento **52A**, 1112 (1967).

<sup>6</sup>G. F. Chew, M. L. Goldberger, F. E. Low, and Y. Nambu, Phys. Rev. **106**, 1345 (1957). Only  $(\vec{\sigma} \cdot \vec{\epsilon})$  contributes to the  $E_{0+}$  amplitude, and the factor 8/3 comes from the evaluation of  $|\langle d | T_1^0 + T_2^0 | d \rangle|^2$ .

<sup>7</sup>C. Bacci, R. Baldini-Celio, C. Mencuccini, A. Reale, M. Spinetti, and A. Zallo, Phys. Letters **28B**, 687 (1969).

<sup>8</sup>F. T. Hadjioannou, Phys. Rev. **125**, 1414 (1962). A

more accurate formula is

$$\frac{d\sigma}{d\Omega} \Big|_{\eta^0 d} = \frac{1}{(4\pi)^2} \left[ \left\langle \frac{w^2}{\epsilon_f \epsilon_f} \right\rangle_{av} \frac{E_i E_f}{W^2} \right] \frac{8}{3} |T^0|_{av}^2 \left( \frac{p^*}{k_{\gamma-d}^*} \right)^2 F^2(q^2)$$

(see Hadjiannou). The quantity in the bracket is  $\approx 1$  and for fixed  $p^*$ ,  $k_{\gamma-d}^* \approx k_{\gamma-p}^*$ .

### CROSS SECTION FOR $\pi^- p \rightarrow \Lambda K^0$ : STRUCTURE NEAR $\Sigma$ THRESHOLD\*

O. Van Dyck, R. Blumenthal, S. Frankel, V. Highland,† J. Nagy,  
T. Sloan,‡ M. Takats, W. Wales, and R. Werbeck

Department of Physics, University of Pennsylvania, Philadelphia, Pennsylvania 19104

(Received 9 June 1969)

The cross section for the reaction  $\pi^- p \rightarrow \Lambda K^0$  has been measured at nine energies from 790 to 1060 MeV, with a beam resolution of  $\pm 1\%$ . The results indicate that a strong, narrow ( $\Gamma \leq 20$  MeV) peak in the cross section lies within the energy bin centered at 893 MeV.

We have measured the threshold-region cross sections for the reaction  $\pi^- p \rightarrow \Lambda K^0$  in a spark-chamber experiment carried out at the Princeton-Pennsylvania accelerator.

A diagram of the apparatus<sup>1</sup> appears in Fig. 1. A beam of negative pions, designed to give a nearly square energy window of 1% half-width, was focused on a 5-cm-long liquid-hydrogen target. An anticoincidence counter and a coincidence hodoscope were used after the target to detect the charged decays from the neutral strange particles. The spark-chamber tracks of the incident pions and the charged decay products were photographed in two 90° stereo views. Approximately 30% of the pictures show an apparent single vee, the majority being from the decay  $\Lambda \rightarrow p\pi^-$ .

The measurement of the pictures was fully automatic. The University of Pennsylvania Hough-Powell flying-spot digitizer processed the 200 000 pictures which were taken in the experiment. The resultant digitizings were processed by a computer program<sup>2</sup> which sought the single vee characteristic of the two-body charged decay of a neutral particle. The program found vee events with 90% efficiency.

Geometric criteria were applied to each event to test the hypothesis that the vee was a  $\Lambda \rightarrow p\pi^-$  decay from  $\Lambda K^0$  production. These criteria required that the reconstructed decay and production vertices were within the fiducial areas, that the decay geometry was compatible with a two-body decay, that stereo pairing by pattern was consistent with stereo pairing by digitizing density, and that the track with the smaller decay

angle, which was assumed to be the proton, was more heavily ionizing.

The kinematic reconstruction is singly constrained if all masses are assumed. The final selection of events was based on limits imposed on the reconstructed incident-pion energy  $T_R$ . Multiple scattering in the apparatus ( $\sim 10$  mrad) and inaccuracy in track fitting reduced the precision of this reconstruction. The full width at half-maximum height of the spectrum of  $T_R$  is 50 MeV. A consequence of this spread is that  $\Lambda$ 's from  $\Sigma^0$  production and decay ( $\pi^- p \rightarrow \Sigma^0 K^0$ ,  $\Sigma^0 \rightarrow \Lambda \gamma$ ) cannot be accurately separated from  $\Lambda$ 's produced directly. In addition the  $\Lambda$  center-of-mass angle cannot be accurately reconstructed.

The  $\Lambda$  yield was defined as the product of the

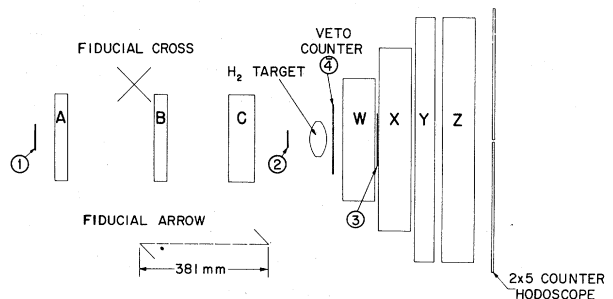


FIG. 1. Apparatus: 1-2 are the beam counters and ABC are spark chambers determining the incident pion line.  $\Lambda$ 's are produced in the 5-cm  $H_2$  target and are required to decay between counters 4 and 3. The charged decay products are observed in spark chambers WXYZ. The hodoscope is a square array two counters high and five counters wide, in which any pair (2/10) were required for the  $\Lambda$  trigger. The complete counter trigger requirement was 1243(2/10).